Exploring the Seasonal Comparison of Land Surface Temperature Dominant Factors in the Tibetan Plateau

Qinghong Sheng[a], Yuejie Zhang[a], Kerui Li[a], Xiao Ling[a], Jun Li[a]

[a] College of Astronautics, Nanjing University of Aeronautics and Astronautics, Nanjing 210016, China
qhsheng@nuaa.edu.cn (Q.H Sheng), zhang_yj@nuaa.edu.cn (Y.J Zhang), lkr151920130@nuaa.edu.cn (K.R Li), xlingsky@nuaa.edu.cn (X. Ling), jun.li@nuaa.edu.cn (J. Li)

Keywords: Land surface temperature, Tibetan Plateau , Driving factors, Seasonal trends, Geodetector.

Abstract

LST (Land Surface Temperature) is a significant parameter that represents the ground energy balance and plays a crucial role in understanding climate change. The LST of the Tibetan Plateau (TP) has a direct influence on the climate and environmental changes of the TP, and it also has a significant impact on global climate and atmospheric circulation. Although there are various factors that drive the spatial and temporal distribution of LST on the TP, the primary driving forces and its seasonal variations of LST are not yet well understood. The research focuses specifically on the TP region, selecting three types of LST data, using geodetector model, to analyze the driving factors affecting the spatial pattern of LST in different seasons. The results indicate that the three factors, Air Temperature (AT), Elevation (Ele), and Permafrost Thermal Stability (PTS), have a significant influence on LST throughout all seasons, whereas other variables demonstrate varying contributions to LST depending on the season. This study contributes to the understanding of the spatial variability of surface thermal conditions and the intricate relationships between their driving factors. It also emphasizes the potential changes in these relationships throughout the year.

1. Introduction

The Tibetan Plateau (TP), an inland plateau in Asia, is the largest plateau in China and the highest in the world. It is also known as the "roof of the world" and the "Third pole". TP rises over 4 kilometers above sea level, creating a barrier that impacts tropospheric circulation and upper air flow over Eurasia. Its distinctive topography is essential for global climate and atmospheric circulation patterns (Oku et al, 2006). Land surface temperature (LST) is a significant factor in the interaction between the surface, near-surface atmosphere, and the water cycle. It is also a vital parameter in the study of ground energy balance and dynamic changes (Anderson et al, 2008; Li et al, 2013). LST directly affects the climate and environmental changes on the TP (Xiao et al, 2015). The LST of the TP is affected by many driving factors. Previous studies have found that the error between LST and its actual value is related to the season and increases with altitude (Salama et al, 2012; Cai et al, 2017). The warming rate increases at low altitudes (4800m and below) but decreases above 5000m (Liu and Chen, 2000; Qin et al, 2009; Zhou et al, 2023). Additionally, changes in vegetation growth significantly impact the surface energy budget (Jeong et al, 2009) and, in turn, surface thermal characteristics, playing a crucial role in LST changes (Bindajam et al, 2020). Over the past 36 years, the amount of atmospheric precipitable water over the TP has been increasing (Lu et al, 2015; Zhang et al, 2013), consistent with the anomaly changes in rising LST (Yao et al, 2015). Clouds (Ma et al, 2020; Pan et al, 2017) and snow (Ghatak et al, 2014; Yang et al, 2021) also contribute to changes in LST. However, it remains unclear which factors among the many influencing factors are the dominant ones.

Examining the driving factors of LST on the TP will aid in comprehending the evolving patterns of LST, enhancing our understanding of the surface-atmosphere exchange process in the region, and effectively addressing the global challenges posed by climate change (Li et al, 2013; Li et al, 2023). However, previous studies have mainly focused on analyzing the impact of single factors on LST, while rarely discussing and analyzing the dominant factors among multiple factors and the ranking of influencing factors, whereas comparing with single factors, the changes in multiple factors have a greater impact on LST. This study aims to address the aforementioned issues by utilizing three types of LST data and multiple driving factors for seasonal analysis. It employs geodetector model (GD) to analyze the spatial heterogeneity of LST and explore the factors influencing this heterogeneity, providing the factors importance ranking. The main objectives of this research are to determine the dominant driving factors and their ranks in different seasons in order to promote regional ecological protection and sustainable development.

2. Study Area and Data

2.1 Study Area

Located in western China, the TP spans between 26°00′~39°47′ north latitude and 73°19′~104°47′ east longitude, covering a total area of approximately 2.5 million square kilometers. Most of TP lies within China and includes all of Tibet and parts of Qinghai, Xinjiang, Gansu, Sichuan and Yunnan (Figure 1-a). The average altitude of the TP ranges from 3000 to 5000 meters, with a majority of the land situated above 4000 meters. The predominant surface types are grassland, which covers 55.9% of the total area, and bare land, which accounts for 35.99%. Forest land is mainly found in the southeast, and the TP also features extensive frozen soil and lakes (Figure 1-b). The climate of the TP is characterized by a typical alpine plateau climate, with intense radiation, abundant sunshine and low air temperatures.

2.2 Data Sources and Pre-processing

In order to ensure more comprehensive research results, three types of LST data are utilized (Table 1), including MYD11A2, Daily 1-km all-weather land surface temperature dataset for Western China V2 (TRIMSAQ) (Zhou et al, 2019), Global

daily average 1km land surface temperature dataset from 2003 to 2019 (GLOBALD) (Zhan et al, 2021). The first is commercially produced satellite products, while the remaining two are independently developed and released by scholars. All there LST data used in this study pertain to the year 2018, and are with the spacial resolution of 1km.

LST data	Spacial resolution	Claimed accuracy
MYD11A2	1 km	1 K
Daily 1-km all-weather land surface temperature dataset for Western China V2 (TRIMSAQ) (Zhou et al, 2019)	1 km	1~3 K
Global daily average 1km land surface temperature dataset from 2003 to 2019 (GLOBALD) (Zhan et al, 2021)	1 km	1~2K

Table 1 LST data used in this study.

Auxiliary data used in this paper include (1) Land Cover data from MODIS MCD12Q1. The original 17 categories are merged into 7 categories (Figure 1-b): 1) Forest land, including: Evergreen Needleleaf Forests, Evergreen Broadleaf Forests, Deciduous Needleleaf Forests, Deciduous Broadleaf Forests, Mixed Forests, Closed Shrublands, and Open Shrublands; 2) Grass land, including: Woody Savannas, Savannas and Grasslands; 3) Farm land, including: Croplands, Cropland/Natural Vegetation Mosaics; 4) Urban area: Urban and Built-up Lands; 5) Snow and Ice: Permanent Snow and Ice; 6) Bare land: Barren; 7) Water body, including: Water Bodies and Permanent Wetlands; (2) Digital Elevation Model from NASADEM (https://search.earthdata.nasa.gov/search); (3) The permafrost thermal stability dataset over TP, released by Ran (Ran et al, 2019); (4) Vegetation Index from MODIS MYD13A2; (5) The 1km daily soil moisture dataset over the TP released by Shangguan (Shangguan et al, 2023); (6) 1-km monthly precipitation dataset for China released by Peng (Peng et al, 2020); (7) 1-km monthly mean temperature dataset for China released by Peng (Peng et al, 2019); (8) China Climate Zone data from the Resource and Environmental Science and Data Center of the Institute of Geographic Sciences and Natural Resources, Chinese Academy of Sciences (https://www.resdc.cn/Default.aspx). The specific details can be found in Table 2. All auxiliary data are resampled to a spatial resolution of 1km to be consistent with the LST data

All data analyses are conducted using ArcGIS 10.8, Python 3.9 and R 4.3.1 (https://www.r-project.org/). The Shapefile data is obtained from the TPBoundary_HF published by Zhang on the National Tibetan Plateau Data Center (Zhang, 2019).

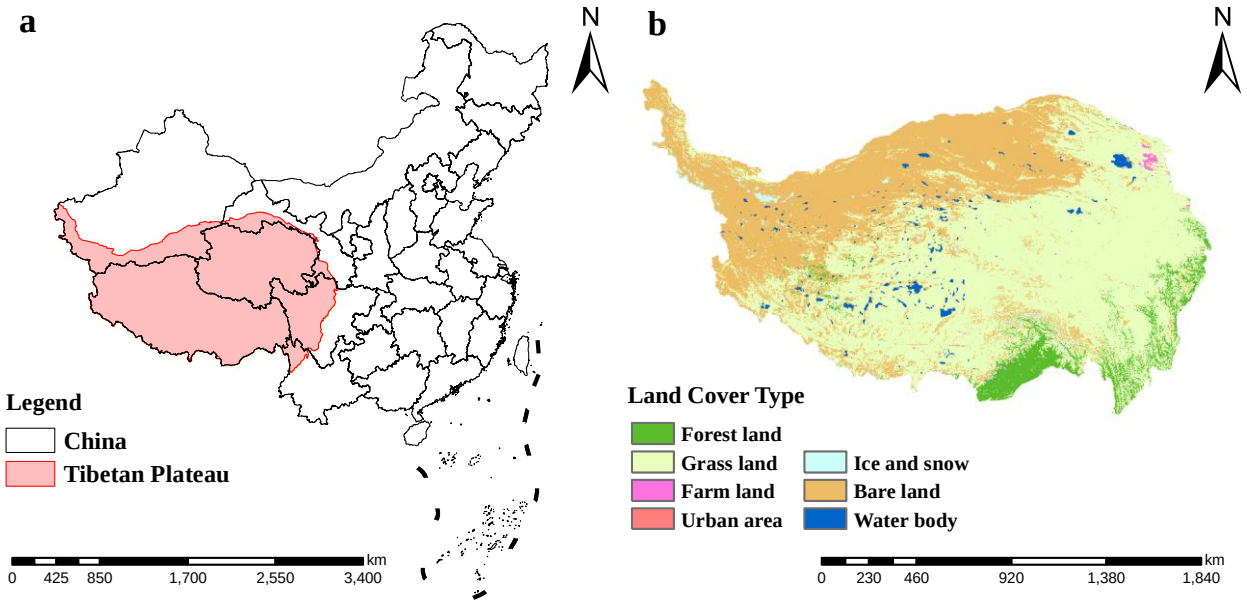

Figure 1. Geographical location of the study area.

3. Methods

3.1 Delineation of Seasons

The TP experiences unique seasonal patterns due to factors such as terrain, altitude, and latitude. It is characterized by a lack of a distinct summer season, with a seamless transition between spring and autumn. Each region within the TP exhibits varying seasonal start and end dates, as well as differing lengths of seasons. For instance, the western Sichuan Plateau experiences an early onset of spring and longer durations of spring, summer, and autumn. Conversely, the central plateau has no distinct summer season due to its higher altitude. In the Yunnan-Guizhou Plateau, spring and autumn are prolonged. These variations in seasonal changes set the TP apart from regions at similar latitudes in China, showcasing its unique climatic characteristics. Fan proposed the 'Universal Plateau Season Division Method' to categorize the four seasons of the TP (Fan et al, 2011). According to this method, winter is defined as the period with an average temperature consistently below 5°C, summer is defined as the period with an average temperature consistently above 15°C, and the seasons with average temperatures between 5°C and 15°C are classified as spring and autumn.

By combining the above conclusions with the actual air temperature changes on the TP in 2018 (Figure 2) and considering the time resolution of LST and Vegetation index data, the four seasons are divided as follows: spring from May 1 to July 3 (64 days); summer from July 4 to August 4 (32 days);

autumn from August 5 to October 7 (64 days); and winter from January 1 to April 30 and from October 8 to December 31 (205 days).

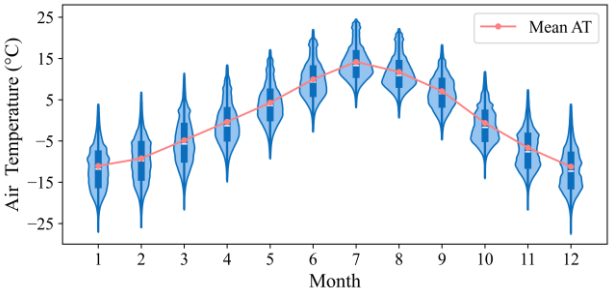

Figure 2. Average monthly air temperature on the TP.

3.2 Influencing Factors Selection

The TP is characterized by its dense coverage of mountains and rivers, featuring steep and ever-changing terrain and complex topography. The LST on the TP is influenced by various factors such as topography, land cover types and vegetation coverage, resulting in a high degree of spatial heterogeneity (He et al, 2019). To assess vegetation coverage, the commonly used indicators are the Enhanced Vegetation Index (EVI) and the Normalized Difference Vegetation Index (NDVI) (Yuan et al, 2007). Additionally, the presence of a significant amount of permafrost across the TP and the unique climate conditions of the TP also impact LST. In the light of the foregoing, this study selected 14 influencing factors, all are obtained from the above auxiliary data (Table 2).

Influencing factors	Auxiliary data obtained from	Spacial resolution	Temporal resolution	Obtained Methods
Land Cover (LC)	MCD12Q1	500m	Yearly	Original obtained through the supervised decision tree classification method, reclassified in this study
Permafrost Thermal Stability (PTS)	The mean annual ground temperature (MAGT) and Permafrost Thermal Stability dataset over Tibetan Plateau for 2005-2015 (Ran and Li, 2019)	1km	10 year	Obtained by fusing ground observations with remote sensing and reanalysis data using a support vector regression model.
Enhanced Vegetation Index (EVI)	MYD13A2	1km	16 day	Obtained from daily atmospherically corrected bidirectional surface reflectance.
Normalized Difference Vegetation Index (NDVI)		1km	16 day	
Soil Moisture (SM)	A 1 km daily soil moisture dataset over the Qinghai-Tibet Plateau (2001-2020) (Shangguan et al, 2023)	1km	Daily	Downscaling the ESA CCI soil moisture data using five machine/deep learning methods, then fusing using the bayesian generalized tricorn hat method.
Elevation (Ele)	NASADEM	30m		Obtained from the improved algorithm of SRTM data, using ASTER GDEM to fill in the missing parts.
Slope (Slp)		30m		
Aspect (Asp)		30m		
Degree of relief (Deg)		30m		
Precipitation (PRCP)	1-km monthly precipitation dataset for China (1901-2022) (Peng, 2020)	1km	Monthly	Generated by downscaling in the Chinese region based on the global 0.5° climate data set released by CRU and the global high-resolution climate data set released by WorldClim through the Delta spatial downscaling scheme.
Air Temperature (AT)	1-km monthly mean temperature dataset for china (1901-2022) (Peng, 2019)	1km	Monthly	
Climate Zone (CZ)	Climate zone data			Divided based on thermal indicators, China's terrain characteristics and historical administrative divisions
Longitude (Lon) Latitude (Lat)	Integration dataset of Tibet Plateau boundary (Zhang, 2019)			Calculated from Shapefile data in ArcGIS and Python.

Table 2 Influencing factors of LST used in this study.

3.3 Statistical Analysis

Geodetector are employed to evaluate the impact of various factors on LST. Geodetectors include four detectors (Wang and Xu, 2017): factor detector, interaction detector, risk detector and ecological detector. Geodetector is available for free at http://www.geodetector.cn/. By considering three LST data as dependent variables, 14 influencing factors as independent variables, this article utilizes factor detector and interaction detector to analyze the independent effects and the joint effects of 14 influencing factors on LST in different seasons. Additionally, the degree of influence and ranking during interactions are examined.

Factor detector can detect the spatial stratified heterogeneity of variable Y and the explanatory power of factor X to the spatial stratified heterogeneity of Y. A *q*-statistic method is proposed to measure the degree of spatial stratified heterogeneity and to test its significance (Wang et al, 2010), The *q*-statistic is defined as follows:

$$q = 1 - \frac{\sum_{h=1}^{L} N_h \sigma_h^2}{N\sigma^2} = 1 - \frac{SSW}{SST}$$
$$SSW = \sum_{h=1}^{L} N_h \sigma_h^2 \qquad (1)$$
$$SST = N\sigma^2$$

where $h = 1, ..., L$ = the stratum for variable Y or factor X
N_h = composing units of stratum h
N = composing units of population
σ_h^2 = stratum variance of stratum h
σ^2 = population variance
SSW = within sum of squares
SST = total sum of squares

The q value is within [0,1], and it increases as the strength of the stratified heterogeneity increases. (0 if a spatial stratification of heterogeneity is not significant, and 1 if there is a perfect spatial stratification of heterogeneity). The q value means factor X explain $100 \times q\%$ of variable Y.

Interaction detector can identify the interaction between different factors X_s and assess whether factors X_1 and X_2 together increase or decrease the explanatory power of the dependent variable Y, or whether the effects of these factors on Y are independent of each other. The evaluation method involves calculating the q values q_1 and q_2 for the two factors X_1 and X_2 with respect to Y individually, and then calculating the q values $q(X_1 \cap X_2)$ when they interact (represented by the new polygon distribution formed by the tangent of the two layers of superimposed variables X_1 and X_2). These values are then compared and the interaction results are given according to the description shown in Table 3.

Description	Interaction
$q(X_1 \cap X_2) < Min(q(X_1), q(X_2))$	Weaken, nonlinear
$Min(q(X_1), q(X_2)) < q(X_1 \cap X_2) < Max(q(X_1), q(X_2))$	Weaken, uni-
$q(X_1 \cap X_2) > Max(q(X_1), q(X_2))$	Enhance, bi-
$q(X_1 \cap X_2) = q(X_1) + q(X_2)$	Independent
$q(X_1 \cap X_2) > q(X_1) + q(X_2)$	Enhance, nonlinear

Table 3 Interaction between Explanatory Variables

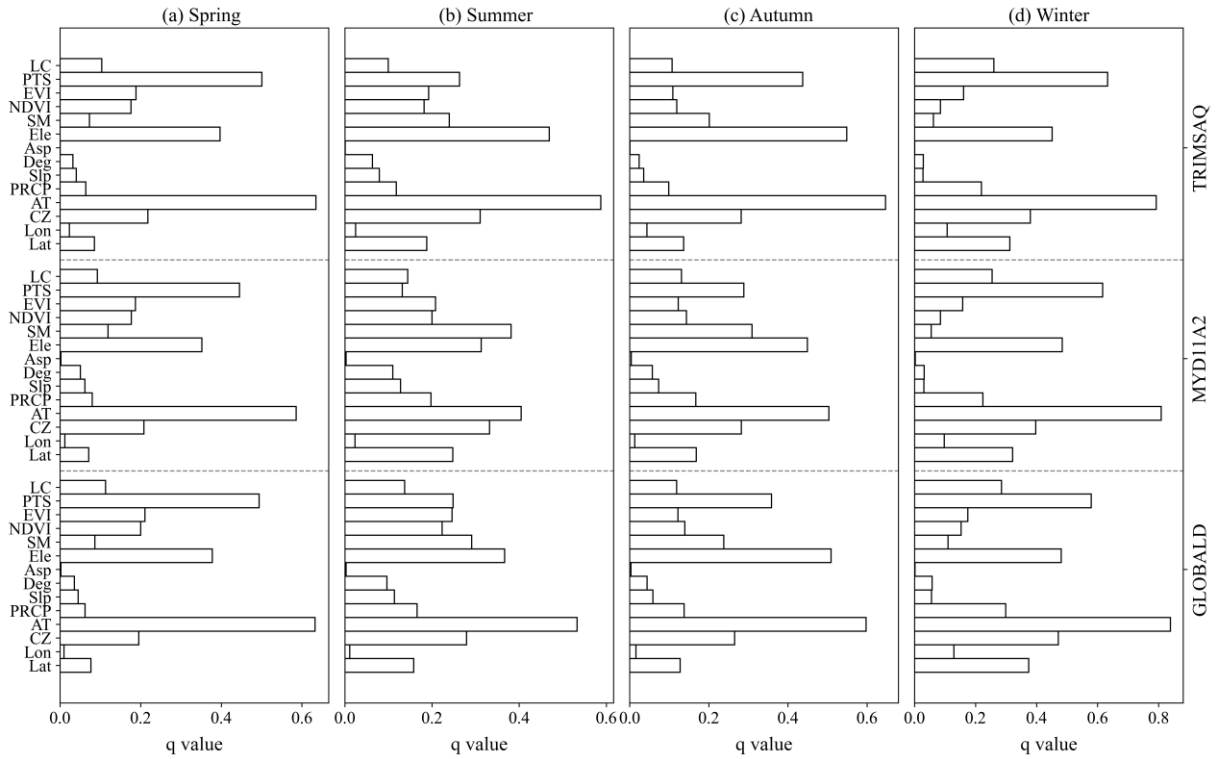

Figure 3. The independent influence of different factors on the LST given by the factor detector in (a) Spring, (b) Summer, (c) Autumn, (d) Winter. (p value for all factors is less than 0.01)

4. Results

4.1 Analysis of Independent Effects of Different Influencing Factors on LST

The results of factor detector are shown in Figure 3. All factors passed the significance test ($p < 0.01$). Since factors with q values less than 0.1 have minimal influence on LST, only factors with q values more than 0.1 for all three kinds of LST data are considered in this article. In the case of spring, the three factors AT, PTS and Ele exhibit strong explanatory power ($q \geq 0.3$) on land surface temperature in all LST data, with average q values of 0.62, 0.48 and 0.38, respectively. Followed by CZ (0.21), EVI (0.20) and NDVI (0.18).

During summer, the four factors AT, Ele, CZ and SM have strong explanatory power on land surface temperature in any LST data. The average q values for the three LST data are 0.51, 0.38, 0.31 and 0.30 respectively. Additionally, EVI (0.22), PTS (0.21), NDVI (0.20) and Lat (0.20) also contribute to explaining LST, with Lat having a higher explanatory power for MYD21A2-LST compared to the other two LST data, while PTS shows the opposite trend.

Autumn shows a similar pattern to spring, with the three factors AT, Ele and PTS, strongly influencing LST in any data set. The average *q* values for the three LST data are 0.58, 0.50 and 0.36 respectively. In addition to these three factors, other variables that significantly impact LST during autumn include CZ (0.28), SM (0.25), Lat (0.14), NDVI (0.13) and LC (0.12).

Moving on to winter, the five factors AT, PTS, Ele, CZ and Lat exhibit the strongest explanatory power for LST in any data set. The average *q* values for the three LST data are 0.81, 0.61, 0.47, 0.42 and 0.34 respectively. Furthermore, LC (0.27) and PRCP (0.25) also contribute to explaining LST during winter.

The results demonstrate that AT, Ele, PTS and CZ significantly impact LST in all seasons. Among these factors, AT has the highest explanatory power for LST in winter (0.81), followed by spring (0.62), autumn (0.58) and summer (0.51). This suggests that the impact of AT on LST diminishes as LST increases. Similarly, PTS has the smallest explanatory power in summer (0.21) and the largest in winter (0.61). Its explanatory power for LST also decreases with higher LST. Additionally, in spring, NDVI and EVI; in summer, SM, EVI, NDVI and Lat; in autumn, SM, NDVI, LC and Lat; and in winter, Lat, LC and PRCP, have a greater influence on LST.

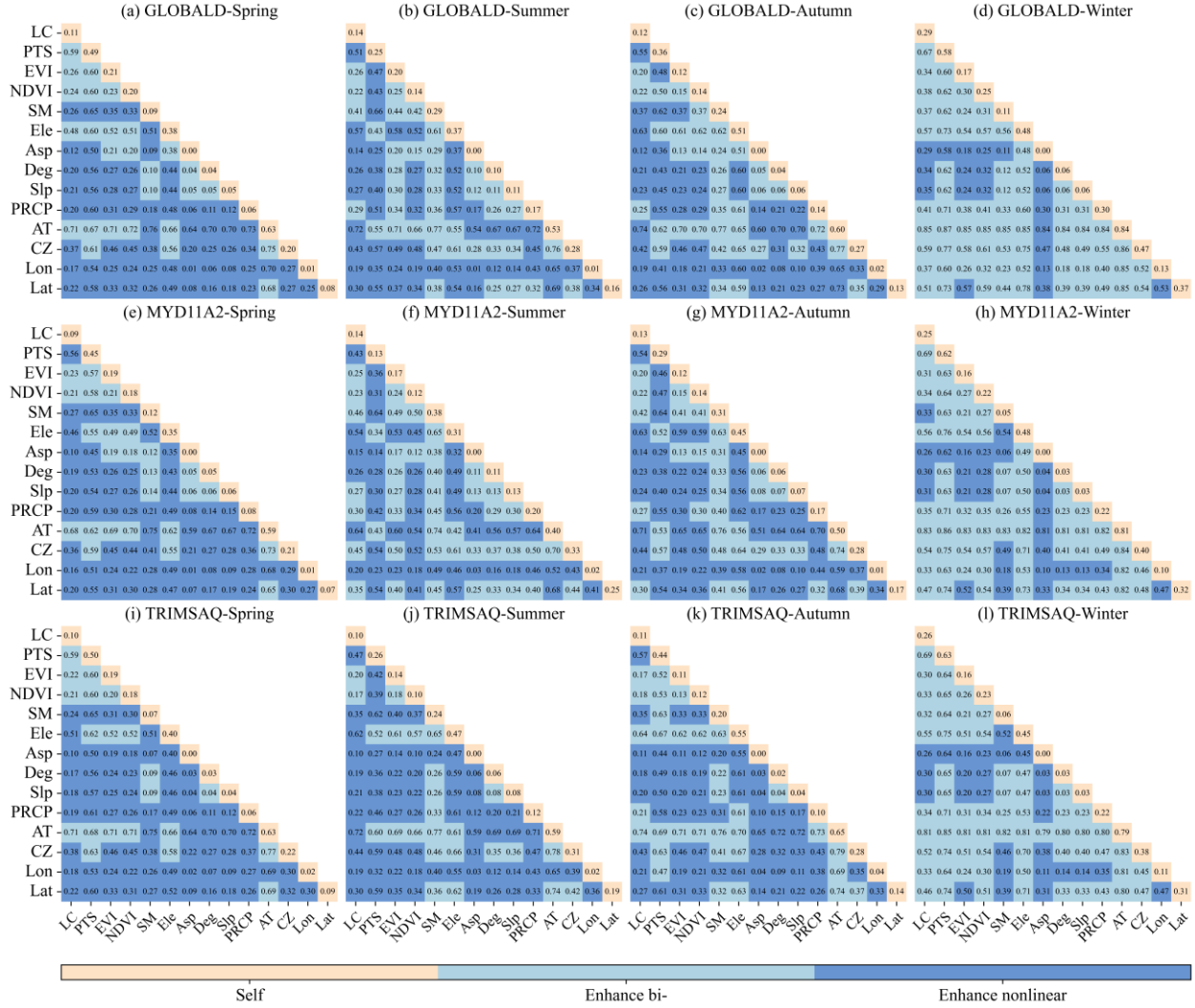

Figure 4. The joint influence of different factors on the LST given by the interaction detector for all three LST data.

4.2 Analysis of Joint Effects of Different Influencing Factors on LST

The study employs interaction detector to examine the interactive effects of influencing factors on LST and evaluate their joint explanatory power. The results (Figure 4) indicate that any pairwise combination of factors has a greater explanatory power for LST compared to individual factors alone. This suggests that the spatial distribution of LST is influenced by multiple factors rather than a single factor. However, the intensity of factor interactions varies across seasons. Non-linear enhancement is dominant in spring, summer and autumn, whereas double-factor enhancement is dominant in winter. This indicates that the influence of interactions is stronger in spring, summer and autumn compared to winter. Similar to the contribution of individual factors, the interaction between air temperature (AT) and other factors is the most significant. In spring, the combination of AT and CZ exhibits the strongest explanatory power for LST (0.74). In summer and autumn, the combination of AT and SM has the highest explanatory power (0.76, 0.77), while in winter, the combination of AT and PTS shows the strongest explanatory power (0.85) for LST. Furthermore, in the analysis of individual factors, the joint

This contribution has been peer-reviewed. The double-blind peer-review was conducted on the basis of the full paper.
https://doi.org/10.5194/isprs-annals-X-1-2024-197-2024 | © Author(s) 2024. CC BY 4.0 License.

effect after pairwise interaction significantly increases for factors with a *q* value less than 0.1 in all four seasons.

5. Discussion

Summary of the main factors influencing LST in each season are provided in Table 4, based on a comprehensive analysis of three types of LST data. The findings indicate that AT and Ele are the most significant factors affecting LST, which aligns with the research conducted by Yang (Yang MJ et al, 2021) and Kerchove (Kerchove et al, 2013). PTS, on the other hand, has received limited attention in previous studies. In this study, we examined the relationship between five thermally stable types of permafrost (extremely stable, stable, substable, transitional, and unstable) and LST. The results revealed that the influence of permafrost's thermal stability on LST weakens as LST increases. This effect is strongest in winter and weakest in summer. Additionally, it is observed that lower thermal stability of permafrost corresponds to higher LST.

Season	1	2	3	4	5	6	7	8
Spring	AT	PTS	Ele	CZ	EVI	NDVI		
Summer	AT	Ele	CZ	SM	EVI	NDVI	Lat	PTS
Autumn	AT	Ele	PTS	CZ	SM	Lat	NDVI	LC
Winter	AT	PTS	Ele	CZ	Lat	LC	PRCP	

Table 4 Main factors influencing LST in each season

Vegetation plays a crucial role in influencing LST changes. It not only controls LST through surface energy balance but also affects the visibility of bare soil and vegetation to the sensor. The difference in radiant temperature between soil and vegetation canopy further impacts the overall LST (Sandholt et al, 2002). Statistical analysis reveals that EVI and NDVI significantly contribute to LST in spring, summer, and autumn, albeit to varying degrees. This indicates that vegetation regulates the spatial distribution of LST, aligning with the findings of Zou's research (Zou et al, 2020).

The impact of soil moisture (SM) on LST is limited during winter due to permafrost, which restricts heat exchange.
Generally, precipitation has a greater influence on LST. However, this study demonstrates that PRCP alone has a relatively minor effect on LST, primarily observed in winter. This is because the monsoon-induced high precipitation during summer leads to increased vegetation coverage and soil moisture (Xu et al, 2013; Wang et al, 2008). As vegetation coverage and soil moisture directly participate in surface heat exchange, the impact of EVI, NDVI, and SM on LST is more significant than that of PRCP. This pattern is consistent in spring and autumn as well.

Referring to published studies, we select 14 influencing factors to analyze their effects on LST. However, Snow cover distribution, albedo and evapotranspiration also affect LST to varying degrees. Interestingly, despite the complex topographic conditions of the TP, only Ele has been found to have a significant impact on LST. Therefore, the effects of influencing factors mentioned above associate with Slp, Asp and Deg on LST would be a good choice to analyze in future studies.

6. Conclusion

In this study, we employ geodetector to investigate the factors driving spatial variations in LST across different seasons. The findings reveal that for each season, air temperature (AT) and elevation (Ele) play a significant role in shaping the spatial patterns of LST. As the LST rises, the impact of permafrost thermal stability (PTS) diminishes, yet it continues to contribute to the LST in all four seasons. Overall, the factors influencing LST in spring and their respective order are: AT > PTS > Ele > CZ > EVI > NDVI; summer: AT > Ele > CZ > SM > EVI > NDVI > Lat > PTS; autumn: AT > Ele > PTS > CZ > SM > Lat > NDVI > LC; winter: AT > PTS > Ele > CZ > Lat > LC > PRCP.

Acknowledgements

The authors would like to thank the National Tibetan Plateau Data Center and the Resource and Environment Science and Data Center, the National Aeronautics and Space Administration(NASA) for providing the data that used in this research.

References

Anderson, M. C., Norman, J. M., Kustas, W. P., Houborg, R., Starks, P. J., Agam, N., 2008: A thermal-based remote sensing technique for routine mapping of land-surface carbon, water and energy fluxes from field to regional scales. *Remote Sensing of Environment*, 112(12), 4227-4241.

Bindajam, A. A., Mallick, J., AlQadhi, S., Singh, C. K., Hang, H. T., 2020: Impacts of vegetation and topography on land surface temperature variability over the semi-arid mountain cities of Saudi Arabia. *Atmosphere*, 11(7), 762.

Cai, D. L, You, Q. L., Fraedrich, K., Guan, Y. N., 2017: Spatiotemporal temperature variability over the Tibetan Plateau: altitudinal dependence associated with the global warming hiatus. *Journal of Climate*, 30(3), 969-984.

Ghatak, D., Sinsky, E., Miller, J., 2014: Role of snow-albedo feedback in higher elevation warming over the Himalayas, Tibetan Plateau and Central Asia. *Environmental Research Letters*, 9(11), 114008.

He, J. L., Zhao, W., Li, A. N., Wen, F. P., Yu, D. J., 2019: The impact of the terrain effect on land surface temperature variation based on Landsat-8 observations in mountainous areas. *International Journal of Remote Sensing*, 40(5-6), 1808-1827.

Jeong, S. J., Ho, C. H., Kim, K. Y., Jeong, J. H., 2009: Reduction of spring warming over East Asia associated with vegetation feedback. *Geophys. Res. Lett.*, 36(18), 18705.

Li, J. H., Li, Z. L., Liu, X. Y., Duan, S. B., 2023: A global historical twice-daily (daytime and nighttime) land surface temperature dataset produced by Advanced Very High Resolution Radiometer observations from 1981 to 2021. *Earth System Science Data*, 15(5), 2189-2212.

Li, Z. L., Tang, B. H., Wu, H., Ren, H. Z., Yan, G. J., Wan, Z. M., Isabel, F. T., José, A. S., 2013: Satellite-derived land surface temperature: Current status and perspectives. *Remote Sensing of Environment*, 131, 14-37.

Liu, X. D., Chen, B. D., 2000: Climatic warming in the Tibetan Plateau during recent decades. *Int. J. Climatol*., 20(14), 1729-1742.

Lu, N., Trenberth, K. E., Qin, J., Yang, K., Yao, L., 2015: Detecting long-term trends in precipitable water over the Tibetan Plateau by synthesis of station and MODIS observations. *J Clim*, 28(4), 1707–1722.

Ma, Q. R, You, Q. L, Ma, Y. J., Cao, Y., Zhang, J., Niu, M. M., Zhang, Y. Q., 2021: Changes in cloud amount over the Tibetan Plateau and impacts of large-scale circulation. *Atmospheric Research*, 249, 105332.

Oku, Y., Ishikawa, H., Haginoya, S., Ma, Y. M., 2006: Recent trends in land surface temperature on the Tibetan Plateau. *Journal of climate*, 19(12), 2995-3003.

Peng, S., 2020. 1-km monthly precipitation dataset for China (1901-2022). National Tibetan Plateau / Third Pole Environment Data Center. https://doi.org/10.5281/zenodo.3185722.

Peng, S., 2019. 1-km monthly mean temperature dataset for china (1901-2022). National Tibetan Plateau / Third Pole Environment Data Center. https://doi.org/10.11888/Meteoro.tpdc.270961.

Qin, J., Yang, K., Liang, S. L., Guo, X. F., 2009: The altitudinal dependence of recent rapid warming over the Tibetan Plateau. *Climatic Change*, 97(01), 321–327.

Ran, Y. H., Li, X., 2019. The mean annual ground temperature (MAGT) and Permafrost Thermal Stability dataset over Tibetan Plateau for 2005-2015. National Tibetan Plateau / Third Pole Environment Data Center. https://doi.org/10.11888/Geogra.tpdc.270672.

Salama, M. S., Van der Velde, R., Zhong, L., Ma, Y. M., Ofwono, M., Su, Z. B., 2012: Decadal variations of land surface temperature anomalies observed over the Tibetan Plateau by the Special Sensor Microwave Imager (SSM/I) from 1987 to 2008. *Climatic Change*, 114(03): 769–781.

Sandholt, I., Rasmussen, K., Andersen, J., 2002: A Simple Interpretation of the Surface Temperature/Vegetation Index Space for Assessment of Surface Moisture Status, *Remote Sensing of Environment*, 79(2–3), 213–224.

Shangguan, Y., Shi, Z., Min, X. 2023: A 1 km daily soil moisture dataset over the Qinghai-Tibet Plateau (2001-2020). National Tibetan Plateau / Third Pole Environment Data Center. https://doi.org/10.11888/Terre.tpdc.300224.

Van, D. K. R., Lhermitte, S., Veraverbeke, S., Goossens, R., 2013: Spatio-temporal variability in remotely sensed land surface temperature, and its relationship with physiographic variables in the Russian Altay Mountains. *International Journal of Applied Earth Observation and Geoinformation*, 20, 4-19.

Wang, B., Bao, Q., Hoskins, B., Wu, G., Liu, Y., 2008: Tibetan plateau warming and precipitation changes in East Asia, *Geophysical Research Letters*, 35(14), 14702.

Wang, J. F., Li, X. H., Christakos, G., Liao, Y. L., Zhang, T., Gu, X., Zheng, X. Y., 2010: Geographical Detectors-Based Health Risk Assessment and its Application in the Neural Tube Defects Study of the Heshun Region, China, *International Journal of Geographical Information Science*, 24(1), 107-127.

Wang, J. F., Xu, C. D., 2017: Geodetector: Principle and prospective, Acta Geographica Sinica, 72(1), 116-134.

Xiao, L., Che, T., 2015: Preliminary Study on Snow Feedback to the Climate System in the Tibetan Plateau. *Remote Sensing Technology and Application*, 30(6), 1066-1075.

Xu, Y., Shen, Y., Wu, Z., 2013: Spatial and temporal variations of land surface temperature over the Tibetan Plateau based on harmonic analysis, *Mountain Research and Development*, 33(1), 85-94.

Yang, M. J., Zhao, W., Zhan, Q. Q., Xiong, D. H., 2021: Spatiotemporal patterns of land surface temperature change in the tibetan plateau based on MODIS/Terra daily product from 2000 to 2018. *IEEE Journal of Selected Topics in Applied Earth Observations and Remote Sensing*, 14, 6501-6514.

Yao, Y. B., Lei, X. X., Zhang, L., Zhang, B., Peng, H., Zhang, J. H., 2016: Analysis of precipitable water vapor and surface temperature variation over Qinghai-Tibetan Plateau from 1979 to 2014. *Chinese Science Bulletin*, 61(13), 1462 – 1477.

Yuan, F., Bauer, M.E., 2007: Comparison of impervious surface area and normalized difference vegetation index as indicators of surface urban heat island effects in Landsat imagery. *Remote Sensing of Environment*. 106 (3), 375–386.

Zhou, J., Zhang, X. D., Tang, W., Ding, L., Ma, J., Zhang, X. 2019: Daily 1-km all-weather land surface temperature dataset for Western China (TRIMS LST-TP; 2000-2022) V2. National Tibetan Plateau / Third Pole Environment Data Center. https://doi.org/10.11888/Meteoro.tpdc.270953.

Zhou, Y. Z., Ran, Y. H., Li, X., 2023: The contributions of different variables to elevation-dependent land surfac temperature changes over the Tibetan Plateau and surrounding regions. *Global and Planetary Change*, 220, 104010.

Zhan, W. F., Hong, F. L., Chen, Y. Y., 2021. Global daily 1km resolution surface temperature daily average temperature product dataset from 2003 to 2019 [DS/OL]. National Ecological Science Data Center. https://doi.org/10.12199/nesdc.ecodb.2016YFA0600200.01.005.

Zhang, Y. W., Wang, D. H., Zhai, P. M., Gu, G. J., He, J. H., 2013: Spatial distributions and seasonal variations of tropospheric water vapor content over the Tibetan Plateau. *J Clim*, 26(15), 5637–5654.

Zhang, Y., 2019. Integration dataset of Tibet Plateau boundary. National Tibetan Plateau / Third Pole Environment Data Center. https://doi.org/10.11888/Geogra.tpdc.270099.

Zou, F., Li, H., Hu, Q., 2020: Responses of vegetation greening and land surface temperature variations to global warming on the Qinghai-Tibetan Plateau, 2001–2016, *Ecological Indicators*, 119, 106867.